PECVD deposition of a-Si:H and μc-Si:H using a linear RF source

Bas B. Van Aken*, Camile Devilee, Maarten Dörenkämper, Marco Geusebroek, Maurits Heijna, Jochen Löffler, Wim J. Soppe
ECN Solar Energy, P.O. Box 1, 1755 ZG Petten, the Netherlands

ABSTRACT

ECN is aiming at the development of fabrication technology for roll-to-roll production lines for high efficiency thin film amorphous and microcrystalline silicon solar cells. The intrinsic layer will be deposited with high deposition rate microwave plasma enhanced chemical vapour deposition. This plasma source, however, is not suitable for the deposition of doped layers. Therefore, we use a novel, linear RF source for the deposition of doped layers. In this RF source, the substrate is electrically disconnected from the RF network. As a result, the ion bombardment onto the substrate is very mild, with ion energies typically < 10 eV. The low ion energies make this source very attractive for surface treatments like passivation of crystalline silicon wafers by thin SiN_x or a-Si layers. In this contribution, we will introduce the novel RF source and discuss the deposition of device quality amorphous and microcrystalline intrinsic Si layers with the novel linear RF source.

Keywords: thin film Si, RF PECVD, amorphous, microcrystalline, roll-to-roll deposition

1 INTRODUCTION

PECVD is commonly used to deposit μc-Si:H and a-Si:H layers for photovoltaic cells. For industrial production, a high deposition rate and minimal handling costs are important criteria. Microwave plasma enhanced chemical vapour deposition (MW-PECVD) can increase the deposition rate significantly, whereas roll-to-roll production decreases the amount of handling of substrates and (half-)product. The Flexicoat300, a joint development of Roth & Rau AG and ECN, combines these two advantages in a roll-to-roll PECVD system with three chambers for Si deposition. The Flexicoat300 will be the heart of a pilot production line for thin film Si solar cells.

In our vision for roll-to-roll production of thin film Si solar cells, steel foil is used as substrate of the solar cells. The stainless steel foil is coated with an insulating barrier layer, back-contact and –reflector, before the active layers are deposited in the Flexicoat300. On top of the Si layers, a transparent conductive oxide is applied. Finally, the layer stack is divided into cells by laser scribing, these cells are monolithically interconnected by printed metallic lines and last the PV module is encapsulated. The research reported in this contribution focuses entirely on the deposition of Si layers.

The intrinsic layer is deposited with MW-PECVD as this combines good layer quality with high deposition rates. However, MW sources are not suitable for doped layer deposition, since parasitic deposition of conductive layers will decrease the microwave power that can be coupled into the plasma. For that reason, we have chosen to use RF-PECVD for the n-type Si and p-type Si growth.

Industrial RF-PECVD systems usually generate the plasma in a capacitive mode, which involves that the grounded substrate is part of the RF network. In such a set-up, the substrate is bombarded by high-energy ions, typically between 10 and 100 eV. These high-energy ions can have a detrimental effect on the structural and electronic quality of the Si layers. Therefore, a novel RF source was developed by Roth & Rau AG with the motivation of lowering the energy of the ion bombardment and of avoiding the need to ground the substrate.

For this novel source, new deposition processes have to be developed for the deposition of doped Si. As we intend to deposit a-Si:H and μc-Si:H layers in the roll-to-roll coater both in single junction and in tandem solar cells, these processes have to cover both amorphous and microcrystalline growth of p-type Si and n-type Si. Although optimal deposition conditions for doped layers can be different from those for intrinsic layers, processes that yield reasonably good intrinsic layers are good starting points for the optimisation of the deposition processes of the doped layers. This

* vanaken@ecn.nl; phone +31 224 564905; fax +31 224 568214; www.ecn.nl/en/zon

Photovoltaic Cell and Module Technologies, edited by Bolko von Roedern, Alan E. Delahoy,
Proc. of SPIE Vol. 6651, 66510C, (2007) · 0277-786X/07/$18 · doi: 10.1117/12.732383

paper reports on our initial experiments on the deposition of amorphous and microcrystalline intrinsic Si with the novel RF source.

2 EXPERIMENT

Intrinsic Si samples have been grown with RF-PECVD in the roll-to-roll coater Flexicoat300. The Flexicoat300 has five vacuum chambers, see Fig. 1, and can handle foils up to 30 cm wide. As both RF and MW sources are linear, they are easily scaled up to allow foils with widths of up to 150 cm. The PECVD chambers are equipped with plasma boxes to prevent oxygen contamination of the deposited layers due to water desorption from the cold walls. The gas locks allow the setting of different pressures in each of the deposition chambers and prevent the contamination of the intrinsic chamber with dopant gasses such as PH_3 and B_2H_6.

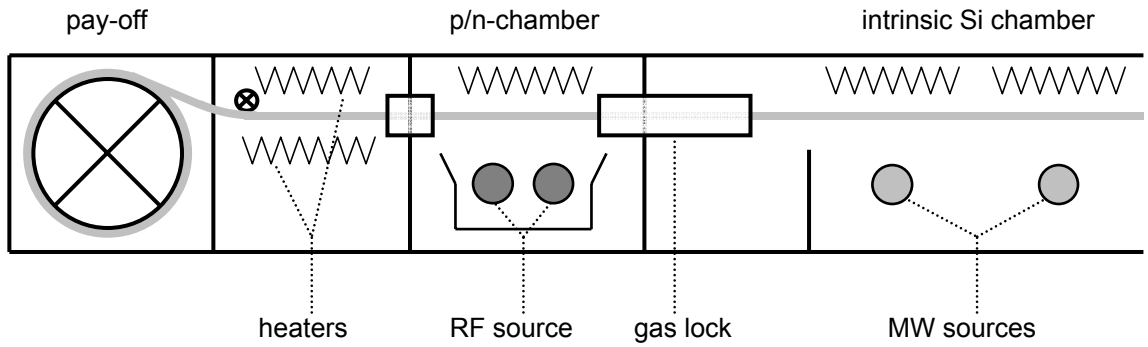

Fig. 1: Cross-section through the Flexicoat300 roll-to-roll coater. For clarity only the left half of the system is shown. The right half is the mirror image with two more MW sources, gas lock, the second p/n-chamber with RF source and a take-up chamber at the end.

The deposition of intrinsic Si in the RF chamber is the first step in developing procedures for doped Si deposition with the novel source. As shown in Fig. 2, the RF electronic network is symmetric. Conventional asymmetric RF sources ignite the plasma between the electrode(s) and all grounded components including the substrate. In contrast, in the symmetric set-up, the plasma is ignited between the two electrodes and the substrate needs not to be grounded.

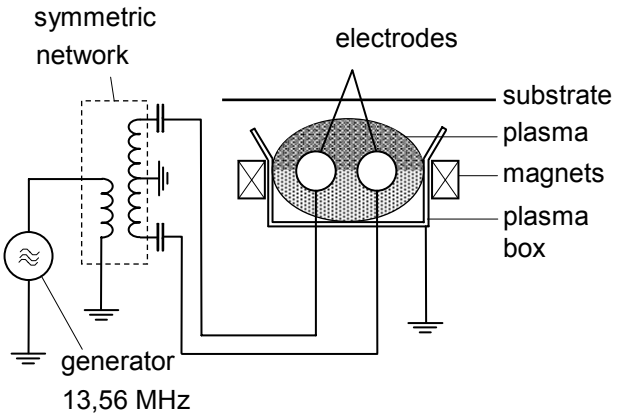

Fig. 2: Sketch of the novel RF source. The RF source can be operated with and without an additional magnetic field. The plasma is ignited between the two electrodes. Depending on the pressure, the plasma has little or no contact with the substrate.

The resulting remote plasma is analysed with a retarding field analyser and a Langmuir probe. The Langmuir probe measures the ion current density at the substrate surface. The retarding field analyser (RFA) is used to determine the energy distribution of the ion bombardment.[1,2] In an RFA, a grid separates the electrons from the positive ions, then the incoming ions are slowed down by a stepwise increased retarding field and the current is measured. The change in

current between consecutive retarding field steps is proportional to the number of ions with an energy corresponding to the retarding field.

Although the Flexicoat300 is designed for continuous roll-to-roll deposition, static depositions on small substrates for research purposes are also possible. For static deposition, an aperture is placed in the plasma box to reduce the deposition area to approximately 3 cm by 30 cm, respectively perpendicular and parallel to the RF electrodes. In these experiments, we typically deposited Si layers on three substrates in one run: one crystalline Si CZ wafer for FTIR measurements and two Corning2000 glass substrates. On one of the layers on a glass substrate, Al contacts are evaporated for two-point conductivity and FTPS experiments.[3] The other layer on glass is used for optical measurements, such as reflectance and transmittance and Raman spectroscopy.

FTIR spectra are recorded with a Perkin Elmer BX II spectrometer. The crystalline fraction is determined by Raman spectroscopy on a Renishaw Raman microscope at 514 nm wavelength at the University of Neuchâtel (Switzerland) and Delft University of Technology (the Netherlands). Dark conductivity is measured with a Keithley-595 quasistatic CV meter; the activation energy of the dark conductivity is calculated from an Arrhenius plot of the dark conductivity against the temperature. For FTPS, a Nicolet 5700 FTIR spectrometer is applied, using a Keithley-2400 source-measure unit to measure the photocurrent. Photoconductivity is recorded in a solar simulator at 1.5 AM also with a Keithley-2400 source-measure unit.

3 RESULTS AND DISCUSSION

3.1 Novel linear RF source

For good quality roll-to-roll deposition of solar cells, uniformity over the width of the foil is required. To analyse if the plasma that is generated with the RF source is uniform, the current density has been measured. Results for one set of deposition conditions, 450 W, 0.1 mbar and a constant hydrogen flow, are plotted in Fig. 3. Because the probes are placed at the position of the substrate, the current density is measured at the substrate surface. The sharp down turns at 0 mm and 300 mm are not due to edge effects of the RF source, which is much longer than these 300 mm, but are caused by the plasma box shadowing part of the substrate and thus of the probes. More to the point, the current density is uniform along the length of the RF source within a few percent.

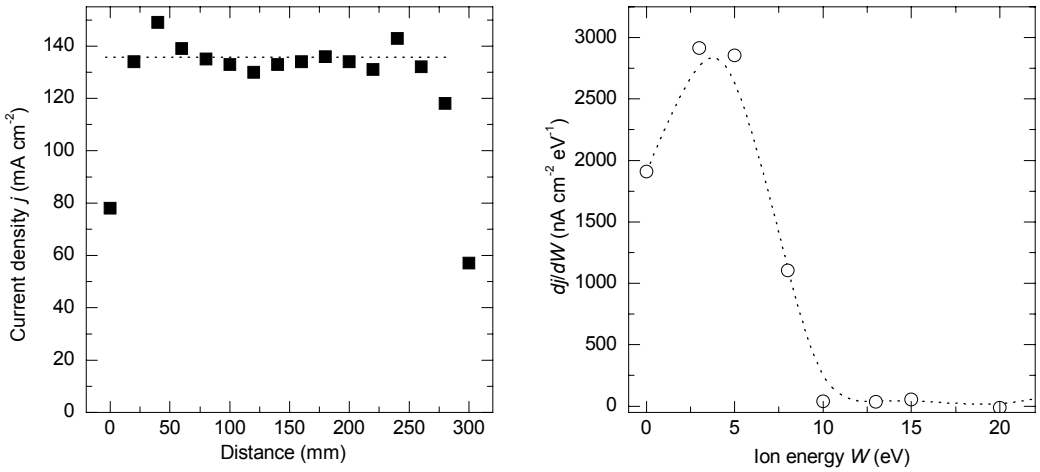

Fig. 3. Plasma characteristics at the sample surface of a H2 plasma at 0.1 mbar and RF power of 450 W. Left: Current density along the length of the RF electrodes. The horizontal line is the average of the central 22 cm. Right: Retarding field analysis of the same plasma in the centre of the electrode. The dashed line is a guide to the eye.

One of the arguments in favour of a symmetric linear RF source is the supposedly mild ion bombardment, reflected in a low energy, as determined by RFA, of the ion bombardment. Typically, the ion energy distribution of an asymmetric RF sources shows a narrow maximum at 7-10 eV, but at higher energies a long tail is observed, extending to 60-100 eV.[4] For the novel symmetric RF source installed in the Flexicoat300, the ion energy distribution is plotted in the right panel of Fig. 3. There is also a narrow maximum in the ion energy distribution, but from 10 eV onwards no significant signal in the ion distribution is observed. Therefore, the novel RF source leads to a very mild ion bombardment on the surface of the substrate. Furthermore, the density of the plasma is uniform within a few percent over the width of the source.

3.2 Deposition of amorphous Si

Amorphous Si is grown in the RF chamber of the Flexicoat300 with low H_2-dilution and relatively high pressure at growth rates of about 0.3 Å/s. After initial process optimisation, FTIR data revealed a good dense layer with refractive index n = 3.3 at 0.5 eV and microstructure factor R^* = 0.18 for a layer of ~400 nm thickness. Conductivity data were also of high quality, resulting in a σ_{ph}/σ_d ratio of almost 10^6 and an activation energy E_{act} = 0.85 eV. The material properties are summarised in Table 1.

Table 1. Material properties of amorphous silicon layers deposited by the novel linear RF source. The device quality data are taken from the textbook by Schropp and Zeman.[5]

Material property	present status	device quality
σ_{dark} [S/cm]	1.8×10^{-11}	$<1.0\times10^{-10}$
σ_{photo} [S/cm]	1.7×10^{-5}	$>1.0\times10^{-5}$
$\sigma_{photo}/\sigma_{dark}$	9×10^{5}	$>10^{5}$
E_{act} [eV]	0.85	≈ 0.85
E_{gap} [eV]	1.7	≤1.8
E_{urb} [meV]	59	<50
n @ 0.5 eV	3.3	≈ 3.5
R*	0.18	<0.10

In Fig. 4 (left side) the FTPS spectrum of this a-Si:H layer is shown. Clearly, a steep decline of the FTPS signal is seen with decreasing energy directly below the a-Si:H band gap at 1.8 eV. Fitting the data to a model for the absorption of a μc-Si:H/a-Si:H mixture,[6,7] yields an Urbach tail energy E_{urb} = 59 meV. The Urbach tail is caused by transitions between the localised tail states on the band edge and the extended states well in the conduction or valence band. The better the quality of the a-Si:H layer is, the lower the number of these localised tail states and the steeper the slope of the absorption just below the band gap is. The Urbach tail energy is defined as the inverse of this slope. Good quality a-Si:H layer has typically an E_{urb} < 50 meV.[3]

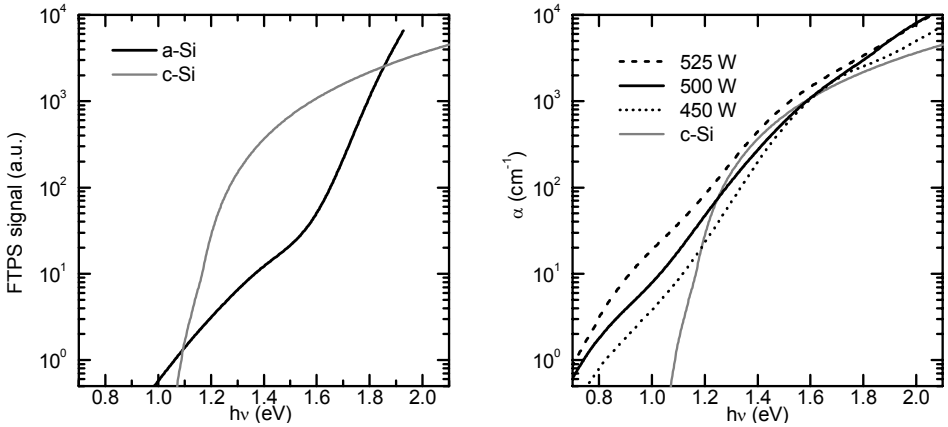

Fig. 4.FTPS spectra of a-Si:H (left) and μc-Si:H (right) thin films. The FTPS curve for c-Si:H is indicated by the grey solid line in both plots. The left data are not scaled to absolute absorption α, due to the absence of reflection and transmission data. The right curve shows FTPS data for films grown with different RF power. Here, the data is scaled to the absolute absorption determined by reflection and transmission experiments. Note the increase of absorption in the range of 1.6-1.9 eV, for higher RF power.

3.3 Transition of a-Si:H to μc-Si:H

One way to achieve the transition of a-Si:H growth to μc-Si:H growth is to increase the H_2-dilution of the process gas in the PECVD chamber. In Fig. 5 left panel, FTIR data is shown for a series of samples with increasing H_2-dilution. The relevant part of the FTIR spectrum is plotted showing the Si-H peaks at 2000-2100 cm^{-1}. Hydrogen passivated dangling bonds in a-Si:H:H contribute to the FTIR spectrum at 2000 cm^{-1}. Hydrogen bonded otherwise, for instance at void surfaces and at grain boundaries, shows up at 2060-2100 cm^{-1}. In particular for single-phase μc-Si:H, where hydrogen is mainly in the grain boundaries, a doublet at 2085 and 2100 cm^{-1} is observed. Using the FTIR spectrum of a bare CZ wafer as (interfering) background, the absorption and refractive index of the layer are determined from a fit of the FTIR spectrum as shown in Fig. 5. We see that for the sample with lowest H_2-dilution most of the intensity is in the 2000 cm^{-1} peak. With increasing H_2-dilution, the 2000 cm^{-1} peak collapses and the peak around 2080 cm^{-1} becomes narrower. These changes indicate the transition from amorphous growth at lower dilution to microcrystalline growth at high dilution.

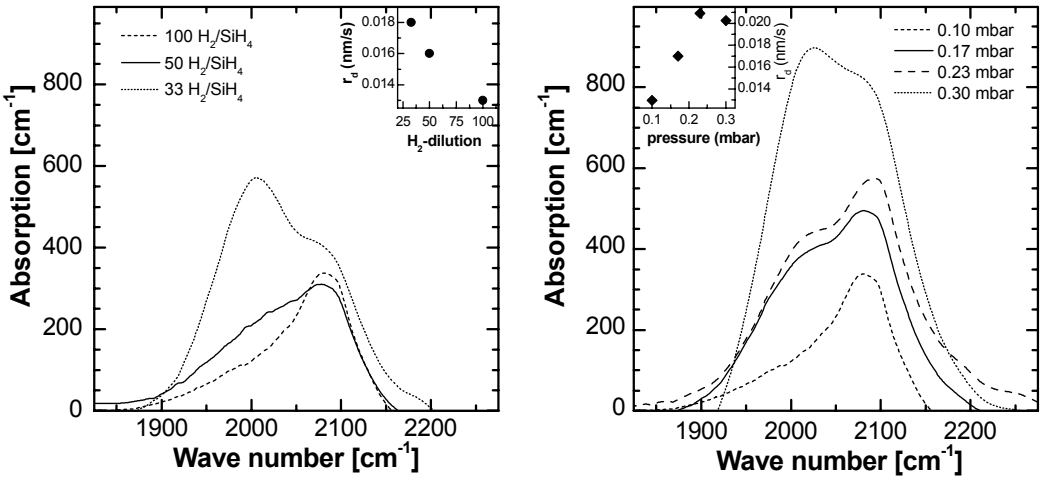

Fig. 5: Absorption derived from the FTIR spectra for two series of thin film Si samples around the amorphous-microcrystalline transition. Left: H_2-dilution series; right: pressure series. In the insets, the growth rate is plotted for the corresponding series.

The a-Si:H to μc-Si:H transition is also observed in a series of samples deposited at various pressures. For the samples deposited at lower pressures a similar curve is observed, see the right side of Fig. 5, as for the higher H_2-dilution samples. With increasing pressure, the FTIR spectrum shifts weight to the 2000 cm^{-1} peak. The increase in the area of the peak with increasing deposition pressure is mostly due to an increase in hydrogen content of the layer from 4% to 12%. We also see that most of the changes take place between the last two samples. This is supported by optical and electronic data. For instance, the band gap determined from a fit to the FTPS data is 1.67 eV for the third sample and 1.79 eV for the last. Furthermore, Raman spectroscopy yielded crystalline fractions of over 70% for the first three samples and less than 10% for the last.

3.4 Microcrystalline Si

Having covered the transition from amorphous to microcrystalline silicon, we now have to evaluate the quality of the microcrystalline layers. In Fig. 4 right panel, FTPS spectra for a series of samples grown under conditions favouring microcrystalline growth are shown. Within the series, the power of the RF source is varied. Compared with the FTPS spectrum of a-Si:H, we observe two major changes. First, the steep decline of the absorption at the a-Si:H band gap is

gone, although a small curvature can still be seen. Second, the absorption below the (μ)c-Si band gap is rather high with a relative shallow decline of the absorption.

Concentrating on the power series, we observe that the FTPS signal above the μc-Si band gap increases with increasing power, suggesting an increase of the crystalline fraction. Furthermore, the FTPS signal below the μc-Si band gap increases too, indicating an increase of the absorption by defects or an increase in the number of localised states at the band edge. This is reflected in the Urbach tail energy of the μc-Si:H phase. The best of these layers, deposited at the highest power, had E_{urb} = 96 meV. Details of this layer are summed up in Table 2.

Table 2. Material properties of microcrystalline silicon layers deposited by the novel linear RF source. The device quality data are taken from the textbook by Schropp and Zeman.[5]

Material property	present status	device quality
σ_{dark} [S/cm]	1.5×10^{-7}	$<1.5\times10^{-7}$
σ_{photo} [S/cm]	4.1×10^{-5}	$>1.5\times10^{-5}$
$\sigma_{photo}/\sigma_{dark}$	267	≈ 100
E_{act} [eV]	0.567	0.53-0.57
n @ 0.5 eV	3.2	>3.4
E_{gap} [eV]		≤1.2
E_{urb} [meV]	96	<50
x_c		>90

The crystalline volume fraction is typically determined with Raman spectroscopy. In the left panel of Fig. 6, the Raman spectrum of a μc-Si:H layer is shown. The spectrum is fitted to three Gaussian peaks and a quadratic background. The sharp peak at 520 cm^{-1} corresponds to the transverse optical mode of crystalline Si. The amorphous phase contributes in the wide peak at 480 cm^{-1}. For small grain sizes, even in "fully" microcrystalline material a significant amount of Si is part of a grain boundary. Therefore, the 520 cm^{-1} peak never has 100% of the intensity and the grain boundaries contribute at lower wave numbers, near ~505 cm^{-1}. The crystalline volume fraction ϕ_c is given by

$$\phi_c = \frac{I_{520} + I_{520}}{I_{520} + I_{505} + mI_{485}}, \tag{1}$$

where I_n is the intensity of the peak at n cm^{-1} and m is a weighting factor for the difference in Raman cross-section of amorphous and microcrystalline silicon and depends on the crystallite size.[8]

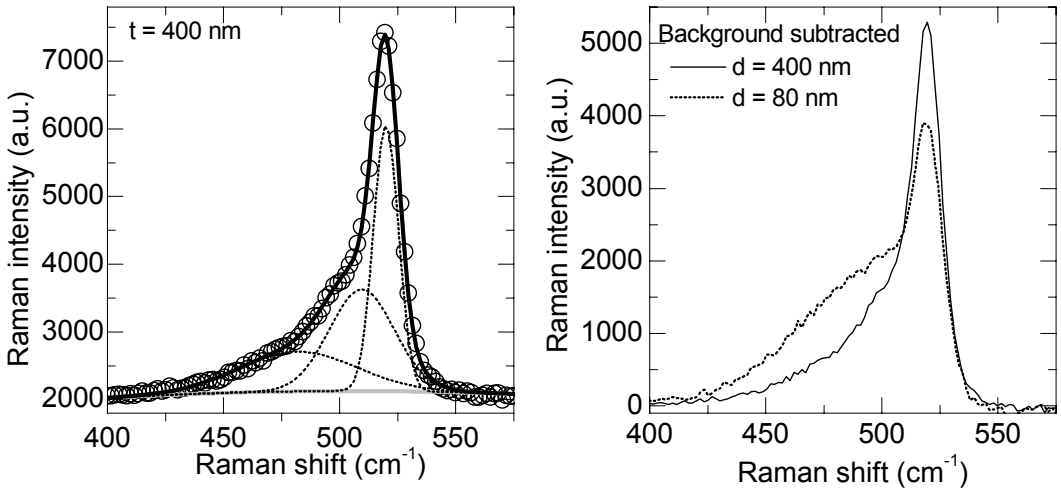

Fig. 6. Raman spectra for a 400 nm and a 90 nm thin film. Left: Raw data for the thicker film is indicated with open circles. The grey solid line indicates the quadratic fit to the background. Three Gaussian peaks, at 520, 505 and 475 cm^{-1}, are fitted to the data and shown as dotted lines. For clarity, these peaks are shown on top of the background. The resulting fit, i.e. quadratic background plus Gaussian peaks, is shown as solid black line. Right: Background corrected data for two films with different layer thickness. Note the shift of intensity from the crystalline peak at 520 cm^{-1} and the grain boundary contribution at 505 cm^{-1} to the broad amorphous peak around 475 cm^{-1} for the thinner film.

The right panel of Fig. 6 shows the Raman spectra for two films grown under the same conditions but with different deposition times and therefore, layer thicknesses. Clearly, the thinner film has more weight at lower wave numbers, corresponding to a decrease in the crystalline volume fraction. After fitting the three-peak model to these curves, we obtained crystalline volume fractions of 88% and 75%, respectively for the 400 nm and 90 nm film.

4 CONCLUSIONS

We have shown that the novel linear RF source exerts a very mild ion bombardment on the surface of the substrate. Typical ion energies are <10 eV and the current density is, within 3%, uniform over the length of the source. This means that the source is well suited for doped Si deposition, but also for other processes that benefit from a very mild ion bombardment, such as passivation of crystalline Si wafers by SiN_x or a-Si layers.

We have shown here that these RF sources are also good for the deposition of intrinsic Si layers. Initial depositions with low H_2 dilution at a high pressure resulted in amorphous silicon layers with an optical band gap of 1.8 eV, a σ_{ph}/σ_d ratio of 9×10^5 and E_{urb} = 59 meV. Typical growth rates are 0.3 Å/s. Since we will use the RF source for deposition of thin doped layers only, this deposition rate is not in unbalance with the proposed rate for MW-PECVD (>1 nm/s) in the Flexicoat300 for continuous production of amorphous silicon solar cells in roll-to-roll mode. Development of p-type and n-type doped amorphous silicon layers, based on these results, is currently in progress.

Experiments with higher H_2 dilution resulted in microcrystalline layers with higher conductivity and activation energies < 0.57 eV, but, thus far, with a too high E_{urb} for application as intrinsic absorber layer. The best of these layers have E_{urb} = 89 meV, E_{act} = 0.31 eV and σ_{ph}/σ_d ratio = 30. These values correlate well with a crystalline fraction > 80% as determined by Raman spectroscopy. Even for layer thicknesses less than 100 nm, we still find ϕ_c > 70%. These layers were grown at rates higher than 0.1 Å/s. Therefore, we consider these layers as a good starting point for development of processes for n-type and p-type μc-Si:H layers with this source.

To conclude: the novel linear RF source, which has good uniformity and a very mild ion bombardment, allows the deposition of qualitatively good layers of both μc-Si:H and a-Si:H at growth rates well-suited for roll-to-roll production of thin film Si solar cells in the Flexicoat300.

ACKNOWLEDGEMENTS

We kindly acknowledge Evelyne Vallat and Sara Edith Olibet (IMT, Neuchâtel, Switzerland) and Kasper Zwetsloot and Miro Zeman (DIMES, Delft, the Netherlands) for Raman measurements. We also want to thank Hermann Schlemm (Roth & Rau AG, Germany) for performing the plasma density measurements and fruitful discussions.

This work has been financially supported by the Dutch Ministry of Economic Affairs (Project No. TSIN3043) and by the European Commission under contract no. FP6-2006-Energy 3-019948.

REFERENCES

1. H. Ch. Paulini and U. Littmark, "A simple and compact retarding field energy analyzer for the characterization of broad ion beams of low energy", Nuclear Instruments and Methods in Physics Research Section B, **58**, 260-265, 1991.
2. B. Szyszka, S. Jäger, J. Szczyrbowski and G. Bräuer, "Comparison of transparent conductive oxide thin films prepared by a.c. and d.c. reactive magnetron sputtering", Surface and Coatings Technology, **98**, 1304-1314, 1998.
3. M. Vanecek and A. Poruba, "Fourier-transform photocurrent spectroscopy of microcrystalline silicon for solar cells", Applied Physics Letters, **80**, 719-721, 2002.
4. H. Schlemm, M. Fritzsche and D. Roth, "Linear radio frequency plasma sources for large scale industrial applications in photovoltaics", Surface and Coatings Technology, **200**, 958-961, 2005.
5. R. E. I. Schropp and M. Zeman, *Amorphous and microcrystalline silicon solar cells – modelling, materials and device technology*, Kluwer Academic Publishers, Dordrecht, the Netherlands, 1998.
6. J. I. Pankove, *Optical processes in semiconductors*, p. 38ff, Prentice-Hall, Inc., Englewood Cliffs, New Jersey, 1971.
7. D. Kovalev, G. Polisski, M. Ben-Chorin, J. Diener and F. Koch, "The temperature dependence of the absorption coefficient of porous silicon", Journal of Applied Physics, **80**, 5978-5983, 1996.
8. E. Bustarret, M. A. Hachicha and M. Brunel, "Experimental determination of the nanocrystalline volume fraction in silicon thin films from Raman spectroscopy", Applied Physics Letters, **52**, 1675-1677, 1998.